

## Self-Assembled Nanosilicon/Siloxane Composite Films

Fotios Papadimitrakopoulos,\*  
Thomas Phely-Bobin, and Peter Wisniecki

Department of Chemistry, Polymer Science Program,  
Nanomaterials Optoelectronics Laboratory,  
Institute of Materials Science,  
University of Connecticut, Storrs, Connecticut 06269

Received February 2, 1998

Revised Manuscript Received October 15, 1998

### Introduction

In recent years, much attention has been focused on composites based on inorganic nanoparticles.<sup>1–3</sup> Recently, our laboratory has reported a method for preparing stable colloidal suspensions of silicon nanoparticles that, when dispersed in gelatin, result in high refractive index (as high as 3.2) nanocomposites with increased transparency in the red part of the visible spectrum.<sup>4,5</sup> With average size of 20 nm and size distribution of about 25%, their blue-shifted absorption is less likely to originate from quantum confinement,<sup>6</sup> but is rather attributed to Mie scattering and local field effects. Particles smaller than  $1/10$  of the wavelength of the transmitted light could potentially suppress Rayleigh scattering, provided agglomeration does not occur.<sup>7</sup> This is particularly important in realizing optical elements from such nanocomposites, a topic of intense research and development in photonic materials and devices.<sup>8</sup>

The main disadvantages of highly filled systems (such as the 50/50 w/w Si/gelatin composite<sup>4,5</sup>) are the difficulties of achieving film uniformity below 1000 Å film thickness and of avoiding concentration fluctuations that contribute to scattering. This has shifted our fabrication strategy to self-assembly, where both film thickness and uniformity can be readily controlled.<sup>9–11</sup> The lack of significant charge density on Si nanoparticles prevented the use of the traditional polyanion–polycation approach utilized to fabricate highly filled polymer/nanoparticle composites.<sup>9–11</sup> However, in an attempt to control the growth of the SiO<sub>x</sub> coatings on

Si nanoparticles, we noticed that under certain conditions the nanoparticles self-assembled on the walls of the glass vials upon standing. Presently, we report a sonication-assisted oxidation process that enables these Si nanoparticles to spontaneously form thin films on glass or quartz substrates from their colloidal suspensions. The rapid initial adsorption of these nanoparticles (which slows down significantly after 3 h) appears to uniformly coat those surfaces with individual nanosilicon particles (ca. 20 nm) and agglomerates (with thicknesses on the order of 50–80 nm). The coverage achieved by this method exhibits a strong potential in suppressing unwanted light scattering, enabling implementation of such films as light outcoupling layers, along with numerous other applications including thin-film transistors, photovoltaics, and sensors.

**Experimental Section.** *Preparation of Colloidal Silicon Suspensions.* The milling and preparation of stable silicon colloids has been described elsewhere.<sup>4,5</sup> A 2 g portion of nanomilled silicon powder was placed in 75 mL of benzoyl peroxide solution (concentration of  $1.79 \times 10^{-4}$  M) in 100% ethanol (AAPER Alcohol & Chemical Co.) in a sealed Erlenmeyer flask and sonicated for 48 h in a Fisher Scientific FS9 ultrasonic cleaning bath to produce a black suspension. The sonicated suspension was then centrifuged at 3000 rpm for 90 min in a Sorvall Superspeed RC2–B centrifuge at room temperature, and the orange supernatant of colloidal silicon nanoparticles was carefully removed and stored in sealed glass containers. The collection of supernatant can be done repeatedly by removing, after centrifugation, the black silicon powder, adding to it 75 mL of fresh benzoyl peroxide solution and sonicating it overnight, although it has been shown that this progressively leads to larger nanosilicon particle sizes.<sup>5</sup> This colloid was found to be stable for many months; however, the sides of its glass container were coated by an ultrathin film of silicon nanoparticles.

The pH of the ethanolic suspensions of Si nanoparticles was measured with an Accumet 1001 Fischer Scientific pH meter equipped with a standard size porous glass electrode equipped with an internal Ag/AgCl reference. Glass or quartz substrates were cleaned using a standard piranha acid solution (7:3 H<sub>2</sub>SO<sub>4</sub>:H<sub>2</sub>O<sub>2</sub>) followed by copious rinsing in deionized H<sub>2</sub>O, dried with compressed air, and stored in 100% ethanol.

*Characterization Techniques.* UV–vis spectra were recorded on a Perkin-Elmer Lambda 3840 array spectrophotometer. Adsorption studies were performed at room temperature (25 °C) where nine glass substrates were immersed in the nanoparticle suspension (at an upright position), inside a sealed polypropylene container. At each time interval, a slide was carefully removed, washed with ethanol, and quickly dried with compressed air before measuring its UV–vis spectrum.

Fourier transform infrared (FTIR) spectroscopic data were obtained from a Nicolet Magna 560 using a TeGeSe detector at 4 cm<sup>-1</sup> resolution. Thin films of Si nanoparticles were deposited or assembled on double-polished Si wafers, coated on both sides with ca. 400 Å of thermally grown SiO<sub>2</sub> (Si oxidation was performed

\* To whom correspondence should be addressed.

(1) Klabunde, K. J. *Free atoms, clusters, and nanoscale particles*; Academic Press: San Diego, 1994.

(2) Moser, W. R. *Advanced catalysts and nanostructured materials: modern synthetic methods*; Academic Press: San Diego, 1996.

(3) Hoch, H. C.; Jelinski, L. W.; Craighead, H. G. *Nanofabrication and biosystems: integrating materials science, engineering and biology*; Cambridge University Press: Cambridge, 1996.

(4) Bhagwagar, D. E.; Wisniecki, P.; Papadimitrakopoulos, F. *Mater. Res. Soc. Symp. Ser.* **1997**, *457*, 439.

(5) Papadimitrakopoulos, F.; Wisniecki, P.; Bhagwagar, D. E. *Chem. Mater.* **1997**, *9*, 2928.

(6) Brus, L. J. *Phys. Chem.* **1994**, *98*, 3575.

(7) Ogawa, T.; Kanemitsu, Y. *Optical properties of low-dimensional materials*; World Scientific: River Edge, NJ, 1995.

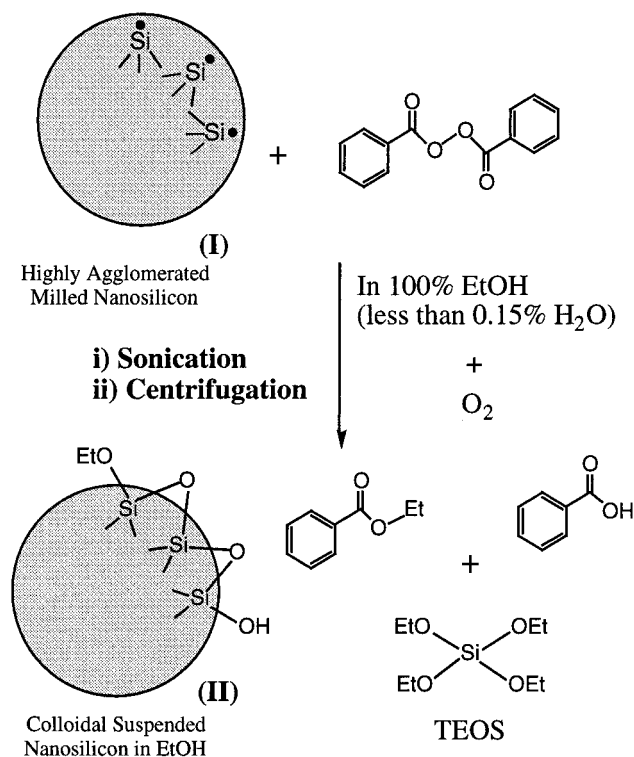
(8) Henneberger, F.; Schmitt-Rink, S.; Gobel, E. O. *Optics of semiconductor nanostructures*; Akademie Verlag: Berlin, Germany, 1993.

(9) Fendler, J. H. *Chem. Mater.* **1996**, *8*, 1616.

(10) Liu, Y.; Wang, A.; Claus, R. *J. Phys. Chem. B* **1997**, *101*, 1385.

(11) Lvov, Y. M.; Rusling, J. F.; Thomsen, D. L.; Papadimitrakopoulos, F.; Kawakami, T.; Kunitake, T. *Chem. Commun.* **1998**, 1229.

### Scheme 1. Schematic Representation of the Sonication-Assisted Oxidation of Silicon Nanoparticles



with dry O<sub>2</sub> at 900 °C for 20 min), and held at 45° with respect to the incident IR beam in order to increase the sampling pathlength and to eliminate the interference fringes from the double-polished silicon wafer. At least 128 scans were signal-averaged. The FTIR spectra of the double-polished SiO<sub>2</sub>/Si/SiO<sub>2</sub> wafers were included into the spectrometer's background to ensure minimum signal contribution from the silicon substrate.

Gas chromatography and mass spectroscopy (GC/MS)-analyses were performed using a HP 6890 series GC system and a HP 6890 series mass selective detector.

Atomic force microscopic (AFM) images were obtained via a Topometrix TMX 2000 Explorer equipped with a liquid cell 12Z scanner of 130 μm *x,y* range and 8 μm *z* range. The sample was immersed in deionized water and its topography was recorded via contact mode (spring constant of 0.082 N/m), from a 5 × 5 μm scan with at a scan rate of 15 μm/s and a resolution of 400 × 400 pixels.

**Results and Discussion.** The formation of stable Si colloids in polar solvents has been attributed to the growth of a thin surface oxide layer.<sup>4,5,12,13</sup> The thickness of such layer has been postulated to be particularly important to enable these relatively large particles to remain suspended,<sup>5</sup> although its minimum value is presently undetermined. Numerous attempts to restrict the moisture-assisted surface oxidation of these nanoparticles, following their milling in an inert atmosphere, have resulted in metastable colloids whose Si nanoparticles uniformly coat the inside wall of their glass

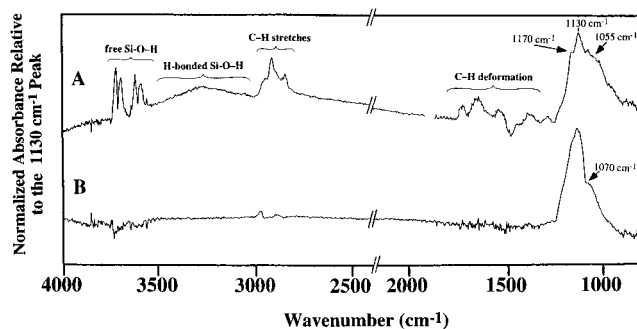


**Figure 1.** FTIR spectra of silicon nanoparticles **II** before (A) and after (B) their assembly on a SiO<sub>2</sub> coated (ca. 400 Å) double-polished silicon substrate. (See the text for details.)

storage container. On the other hand, if moisture was allowed to come in contact with the milled nanoparticles, their colloidal suspensions in ethanol were stable for over 2 years and did not adsorb to glass. With this in mind, a number of oxidizing agents were investigated by utilizing sonication in 100% ethanol (H<sub>2</sub>O concentration < 0.15%). The high energies achieved during sonication, apart from keeping the nanoparticles suspended in EtOH, also provide the means for performing chemistry, in the presence of oxidizing agents such as benzoyl peroxide or 3-chloroperbenzoic acid.<sup>14,15</sup> A small amount of benzoyl peroxide ( $1.79 \times 10^{-4}$  M) was found to produce the optimum results in terms of concentration of Si nanoparticles.

Scheme 1 illustrates the chemistry performed during sonication as analyzed by GC/MS of the silicon colloid and FTIR spectroscopy. The presence of benzoic acid, benzoyl ethyl ester, and tetraethoxysilane (TEOS), along with unreacted benzoyl peroxide, indicate that sonication can provide a considerable amount of energy not only to perform chemical reactions, such as the cleavage of benzoyl peroxide and the formation of benzoic acid and benzoyl ethyl ester but also convert some of the milled Si to TEOS.<sup>17,18</sup>

Figure 1A illustrates the FTIR spectrum of silicon nanoparticles **II**, subjected to three consecutive centrifugation/decantation/resuspension cycles to remove all reactants, and products of Scheme 1 that are not bonded to nanoparticles. The underlying reactions of Scheme 1 facilitate the controlled release of H<sub>2</sub>O, which in turn slowly oxidizes the surface of the Si nanoparticles, forming Si-OH and Si-O-Si groups.<sup>16</sup> The silanol (SiOH) groups are witnessed with two doublets centered around 3712 and 3612 cm<sup>-1</sup> (associated with non-hydrogen-bonded Si-O-H stretching) along with a much broader peak, centered around 3300 cm<sup>-1</sup>, from the hydrogen-bonded Si-O-H stretching. At present, the origin of the two clearly resolved Si-O-H doublets is not entirely understood. Parameters such as the degree of association (between the neighbor SiOH and SiOH/SiOEt groups), the number of OH substitutions (single vs geminal OH groups), variety in fractured crystal planes during nanomilling, and the degree of

(14) Suslick, K. S.; Fang, M.; Hyeon, T. *J. Am. Chem. Soc.* **1996**, *118*, 11960.

(15) Suslick, K. S.; Hyeon, T.; Fang, M. *Chem. Mater.* **1996**, *8*, 2172.

(16) Liao, W. S.; Lee, S. C. *J. Appl. Phys.* **1996**, *80*, 1171.

(17) Mawhinney, D. B.; Glass, J. A.; Yates, J. T. *J. Phys. Chem. B.* **1997**, *101*, 1202.

(18) Hoffmann, P.; Knozinger, E. *Surf. Sci.* **1987**, *188*, 181.

(12) Littau, K. A.; Szajowski, P. J.; Muller, A. J.; Kortan, A. R.; Brus, L. E. *J. Phys. Chem.* **1993**, *97*, 1224.

(13) Bley, R. A.; Kauzlarich, S. M.; Davis, J. E.; Lee, H. W. H. *Chem. Mater.* **1996**, *8*, 1881.

surface oxidation could affect the spectral signature of the Si–O–H stretching mode.<sup>17–19</sup> The strong absorption envelope between 1170 and 1050  $\text{cm}^{-1}$ , originates from Si–O–Si and Si–O–C stretching modes.<sup>16,20</sup> The shoulders at 1170 and 1055  $\text{cm}^{-1}$  correspond to ethoxysiloxane (SiOEt) groups (1170  $\text{cm}^{-1}$  for the  $\text{CH}_3$  rocking absorption and 1055  $\text{cm}^{-1}$  for the Si–O–Si stretching of  $\text{Si}(\text{OEt})_n$  ( $n = 1, 2, 3$ ) groups).<sup>20</sup> The strong absorptions associated with C–H stretching (between 2975 and 2850  $\text{cm}^{-1}$ ) and C–H deformation (five peaks between 1700 and 1300  $\text{cm}^{-1}$ ) are additional evidence for the presence of ethoxysiloxane groups on the surface of these nanoparticles.<sup>19</sup>

The thermally grown oxide on the double-polished silicon substrate allows these nanoparticles to self-assemble on both sides, resulting in highly uniform films. Figure 1B depicts the FTIR spectrum of a 12 h. grown film. The relatively strong adhesion of these nanoparticle assemblies to the substrate prevent them from been lifted off during subsequent washing in fresh ethanol to remove all reactants and products of Scheme 1 that are not bonded to these assemblies. The significant reduction of the shoulders at 1170 and 1055  $\text{cm}^{-1}$  indicates the formation of a  $\text{SiO}_x$  network (1030 and 1070  $\text{cm}^{-1}$ ) at the expense of the ethoxysiloxane groups.<sup>21</sup> This is also confirmed by the disappearance of both free and hydrogen-bonded SiOH groups along with a dramatic reduction in absorbance of the C–H stretching ( $\sim 2900 \text{ cm}^{-1}$ ) and C–H deformation (1700–1300  $\text{cm}^{-1}$ ) peaks.<sup>22</sup>

The formation of a  $\text{SiO}_x$  network is strongly dependent on the pH of the ethanolic suspension.<sup>23–25</sup> The generation of benzoic acid (see Scheme 1) lowers the pH of the nanosilicon suspensions to  $5.0 \pm 0.5$ . At this range, the hydrolysis of TEOS and the ethoxysiloxane groups on the nanoparticles tends to be faster than the condensation of silanol groups to silica.<sup>23,24</sup> On the other hand, the surface oxidation of Si nanoparticles keeps the  $\text{H}_2\text{O}$  concentration in these suspensions sufficiently low, which corroborates with the presence SiOEt groups at this pH (see Figure 1A). In addition, at pH of 5, the partial protonation of the ethoxysiloxane groups decorates these nanoparticles with a positive surface charge, which contributes to the stability of their suspensions.<sup>24,25</sup> Upon immersion of a fresh silica surface (glass or quartz substrates) in these suspensions, the following mechanisms are set in gear.

(i) The weaker nucleophilicity of SiOH and SiOSi groups (present at the surface of glass or quartz substrates) versus the SiOEt groups (on the nanoparticles) makes these substrates less prone to protonation at pH of 5.<sup>24,25</sup> This offers a plausible mechanism that accounts for why nanoparticles of **II** are not repelled

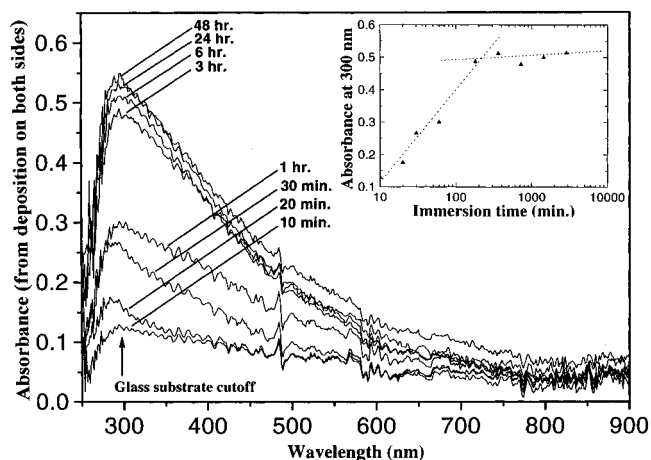


**Figure 2.** UV–vis absorption spectra of self-assembled Si/SiO<sub>x</sub> nanocomposites on both sides of glass substrates as a function of immersion time in a colloidal suspension of **II**.

away from the surface of these substrates.

(ii) Upon substrate–nanoparticle contact, the slow condensation of silanol groups results in the formation of Si–O–Si bridges and generation of additional  $\text{H}_2\text{O}$ . At pH of 5, this  $\text{H}_2\text{O}$  will further promote the fast hydrolysis of SiOEt groups (from nanoparticles as well as TEOS) to SiOH groups, eventually to yield a  $\text{SiO}_x$  matrix around the nanoparticles.<sup>23–25</sup> This is further corroborated by the complete elimination of the Si–O–H stretching in Figure 1B, which creates the slightly negative free Si–O–H absorption ( $\sim 3735 \text{ cm}^{-1}$ ) as a result of substrate SiOH groups, which participate to this condensation (note that the FTIR spectra of double-polished  $\text{SiO}_2/\text{Si}/\text{SiO}_2$  wafers were included into the spectrometer's background).<sup>20</sup>

Figure 2 illustrates the UV–vis absorption spectra of the adsorbed Si/SiO<sub>x</sub> nanocomposite on glass substrates as a function of immersion time in a colloidal suspension of **II**. The rapid initial adsorption of this nanocomposite slows beyond 3 h immersion time, revealing what appears to be a self-limiting deposition process. The optical quality and uniformity of such deposits are impressive, providing a scatter-free coating on glass and quartz substrates. However, after 12 h of immersion time, this coating begins to exhibit some scattering, which can be witnessed at the red spectral portion of Figure 2.

Figure 3 illustrates a typical (contact mode) atomic force micrograph of the adsorbed Si/SiO<sub>x</sub> nanocomposite on glass substrate<sup>26</sup> after 6 h of immersion in the colloidal suspension of **II**. The presence of streaks originates from weakly bound nanoparticles that were caught up by the scanning AFM tip. These streaks can be suppressed but not eliminated by scanning underwater. When the topography was scanned under tapping mode, the resolution was severely compromised, mainly due to electrostatic attraction between the AFM tip and nanoparticles. As shown in the magnified area of Figure 3, individual nanosilicon particles ( $\sim 20 \text{ nm}$ ) seem to uniformly cover the area between the large aggregates. The organization of these nanoparticles is induced by the striations present on the glass substrate,

(26) Please refer to Figure A of the Supporting Information, which depicts a typical contact-mode atomic force micrograph of the glass substrates used in this study.

(19) Tedder, L. L.; Lu, G.; Crowell, J. E. *J. Appl. Phys.* **1991**, *69*, 7037.

(20) Deshmukh, S. C.; Aydil, E. S. *J. Vac. Sci. Technol.* **1995**, *A 13*, 2355.

(21) Ishii, K.; Ohki, Y.; Nishikawa, H. *J. Appl. Phys.* **1994**, *76*, 5418.

(22) Bao, T. I.; Wu, M. S.; I, L. *J. Appl. Phys.* **1995**, *78*, 3342.

(23) Keefer, K. D. In *Silicon-Based Polymer Science: A Comprehensive Resource*; Zeigler, J. M., Gordon-Fearon, F. W., Ed.; American Chemical Society: Washington, 1990; Vol. 224.

(24) McNeill, K. J.; DiCaprio, J. A.; Walsh, D. A.; Pratt, R. F. *J. Am. Chem. Soc.* **1980**, *102*, 1859.

(25) Pohl, E. R.; Osterholtz, F. D. In *Molecular Characterization of Composite Interfaces*; Ishida, H., Kumar, G., Ed.; Plenum Press: New York, 1983; Vol. 27.



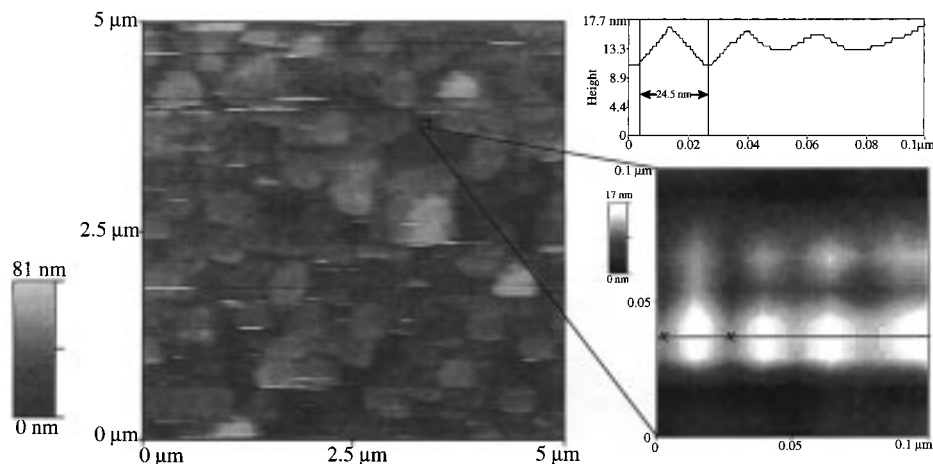


**Figure 3.** Atomic force micrograph of self-assembled Si/SiO<sub>x</sub> nanocomposite on glass substrate after a 6 h immersion in a colloidal suspension of **II**. The magnified area illustrates individual nanosilicon particles and their profile, as they lay between the large aggregates.

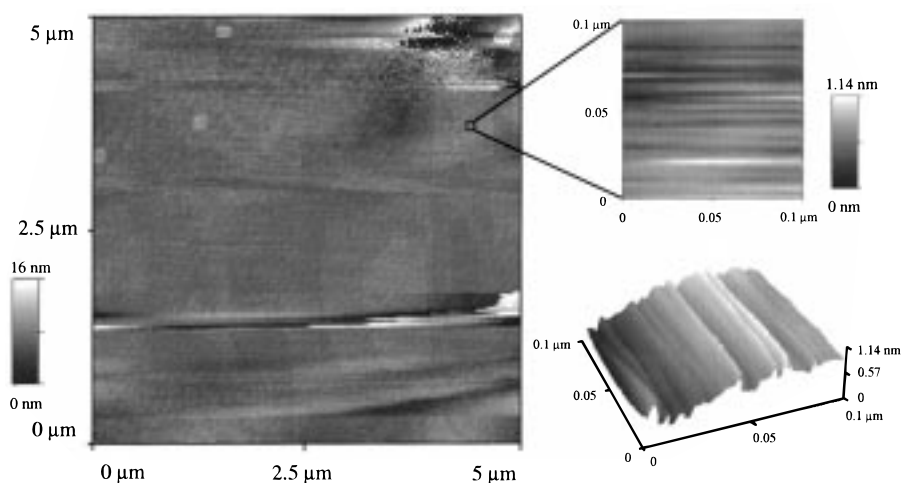


**Figure 4.** Typical contact-mode atomic force micrograph of the background glass substrate used to grow the Si/SiO<sub>x</sub> nanocomposites shown in Figure 3. The magnified area illustrates the striated surface, which is responsible for lining up the nanoparticles depicted in Figure 3.

as shown in Figure 4. The aggregates appear quite smooth and uniform in thickness (ca. 50–80 nm) and most of the times are featureless on magnification. This is attributed to the SiO<sub>x</sub> matrix that surrounds the nanosilicon particles, as evident by FTIR. The formation of these large aggregates is at present speculated to be the result of localized H<sub>2</sub>O formation from silanol condensation. The newly formed H<sub>2</sub>O rapidly hydrolyzes the nearby ethoxysiloxane groups and further facilitates the deposition of new nanoparticle on the growing aggregate. Once the system is depleted of water, it leaves the surface of the SiO<sub>x</sub> matrix terminated with ethoxysiloxane groups, which at pH of 5 are lightly protonated, repelling the condensation of additional nanoparticles. This offers a plausible mecha-

nism for the abrupt change in the rate of Si nanoparticle deposition, as indicated in the inset of Figure 2, although H<sub>2</sub>O starvation of the system cannot be excluded at this time. The nature of this self-assembly process is currently under investigation.

**Acknowledgment.** The authors would like to thank Dr. J. Chen and Prof. F. Jain for helpful discussions. Financial support from NSF Grant ECS 9528731 and the Critical Technologies Program through the Institute of Material Science, University of Connecticut are greatly appreciated.

CM9800579